U.S. DEPARTMENT OF ENERGY | Office of Science

DOE/SC-ARM-TR-293

MOSAiC Radar b1 Processing: Corrections, Calibrations, and Processing Report

A Matthews
E Schuman
S Matrosov
SE Giangrande
K Johnson
Y-C Feng
J Comstock

December 2023

ARM

DISCLAIMER

This report was prepared as an account of work sponsored by the U.S. Government. Neither the United States nor any agency thereof, nor any of their employees, makes any warranty, express or implied, or assumes any legal liability or responsibility for the accuracy, completeness, or usefulness of any information, apparatus, product, or process disclosed, or represents that its use would not infringe privately owned rights. Reference herein to any specific commercial product, process, or service by trade name, trademark, manufacturer, or otherwise, does not necessarily constitute or imply its endorsement, recommendation, or favoring by the U.S. Government or any agency thereof. The views and opinions of authors expressed herein do not necessarily state or reflect those of the U.S. Government or any agency thereof.

DOE/SC-ARM-TR-293

MOSAiC Radar b1 Processing: Corrections, Calibrations, and Processing Report

A Matthews, Pacific Northwest National Laboratory (PNNL)
K Johnson, Brookhaven National Laboratory (BNL)
E Schuman, PNNL
Y-C Feng, PNNL
S Matrosov, National Oceanic and Atmospheric Administration
J Comstock, PNNL
SE Giangrande, BNL

December 2023

How to cite this document:

Matthews, A, K Johnson, E Schuman, Y-C Feng, S Matrosov, J Comstock, and SE Giangrande. 2023. MOSAiC Radar b1 Processing: Corrections, Calibrations, and Processing Report. U.S. Department of Energy, Atmospheric Radiation Measurement user facility, Richland, Washington. DOE/SC-ARM-TR-293.

Work supported by the U.S. Department of Energy,
Office of Science, Office of Biological and Environmental Research

Acknowledgments

This research was primarily supported by the Office of Biological and Environmental Research of the U.S. Department of Energy as part of the Atmospheric Radiation Measurement (ARM) user facility, an Office of Science scientific user facility.

Acronyms and Abbreviations

ARM	Atmospheric Radiation Measurement
CACTI	Cloud, Aerosol, and Complex Terrain Interactions
COMBLE	Cold-air Outbreaks in the Marine Boundary Layer Experiment
DOE	U.S. Department of Energy
eRCA	corner reflector scans
GE	general mode
HSRHI	hemispherical range height indicator scan
KASACR	Ka-band Scanning ARM Cloud Radar
KAZR	Ka-band ARM Zenith Radar
MD	moderate mode
MOS	ARM site code for MOSAiC
MOSAiC	Multidisciplinary Drifting Observatory for the Study of Arctic Climate
MWACR	Marine
NSA	North Slope of Alaska
PPIV	plan position indicatory scan
RF	radio frequency
RV	Research Vessel
SNR	signal-to-noise ratio
XSACR	X-band Scanning ARM Cloud Radar

Contents

Figures

Tables

1.0 Introduction

The U.S. Department of Energy's (DOE) Atmospheric Radiation Measurement (ARM) user facility deployed many instruments on board a German ice breaker, the *Research Vessel (RV) Polarstern*, for one year from October 2019 to October 2020. The purpose of the Multidisciplinary Drifting Observatory for the Study of Arctic Climate (MOSAiC) field campaign was to study the decline in the sea-ice pack around the North Pole, and what factors may be at play. After the campaign ended, efforts were undertaken to provide a calibrated radar data set for future studies. MOSAiC presented new challenges to this process, as existing methodologies often were not applicable for the frozen environment with little to no ground clutter, and concurrent engineering updates or calibrations could not be accomplished once the ship set off (Figure 1).

Like the previous Cloud, Aerosol, and Complex Terrain Interactions (CACTI) and Cold-air Outbreaks in the Marine Boundary Layer Experiment (COMBLE) documentation (Hardin et al. 2020, Matthews et al. 2023), the data correction and calibration process is known in ARM as creating a "b1" datastream. This means that the radar datastreams have been well characterized to the best possible quality. This report will detail the status of the raw "a1" level data sets during the MOSAiC campaign, the corrections that were applied to create the "b1" data files, and the details of the applied methods.

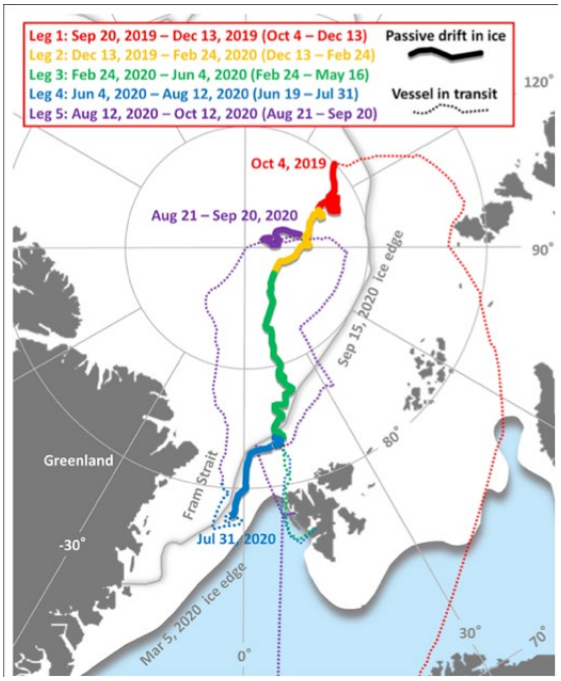

Figure 1. Path of the *RV Polarstern* (Shupe et al. 2022.)

1.1 Overview of the MOSAiC Radars

To accomplish the goals of the cloud and precipitation science theme for MOSAiC (ARM site code MOS), four radars were deployed on board the *Polarstern*. These were the co-mounted Ka-band Scanning ARM Cloud Radar (KASACR) and X-band Scanning ARM Cloud Radar (XSACR), the Ka-band ARM

Zenith Radar (KAZR), and the Marine W-band ARM Cloud Radar (MWACR). The vertically pointing KAZR and MWACR were installed near the bow of the ship, while the Ka/XSACR was installed closer to mid-ship, about 14 meters away and 8.7 meters higher. Figure 2 shows images of the radars at their locations on the ship. The specifications for these radars can be found in Table 1. Unfortunately, shortly after installation the XSACR failed and was unable to be revived in time for the ship launch, and thus did not provide data for this campaign.

Figure 2. ARM radars installed on the *RV Polarstern* for MOSAiC (flickr).

Table 1. Radar specifications during the MOSAiC field campaign.

Radar	*Frequency* (GHz)	*Wavelength* (mm)	*Transmit power* (kW)	*Antenna diameter* (m)	*Beam width* (deg)	*Gate spacing* (m)	*Polarization*
MWACR	95	3.15	1.5	3	0.33	17.48	Horizontal
KASACR	35.3	8.5	2	1.82	0.33	49.96	Horizontal
KAZR	34	8.57	0.187	2	0.3	29.98	Single

1.2 Overview of b1 Processing

As shown in the previous CACTI and COMBLE b1 reports, b1 processing typically focuses on using only a single instrument, although comparisons with other instruments may be done, to avoid excessive merging of ARM datastreams. This section will cover the steps taken for the MOSAiC radar corrections at a high level, before describing each step in more detail. A flow chart of b1 efforts is shown in Figure 3.

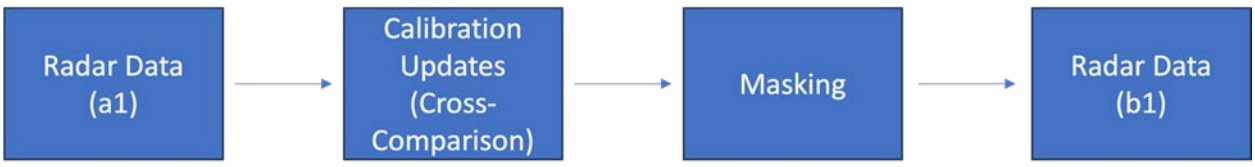

Figure 3. Radar b1 computational flowchart.

1.2.1 Calibration

The primary purpose of the b1 processing is the calibration of the radar datastreams. The calibration of a radar can drift in a variety of ways. The primary function of calibration is to fix the value of the radar constant, C. This constant affects nearly all power measurements the radar takes and represents one of the most dominant sources of errors for the radar. Fundamentally, the radar constant is used as:

$$Z(r_i) = P_r(r_i) - C + 20log_{10}(r_i)$$

Where Z is the radar reflectivity, P is the radar power, and r is the range. The radar constant C is made up of numerous terms including the finite filter loss, the gain of the antenna, and the wavelength. We can, however, represent it as a constant. Once the constant is solved for, correcting calibration is a linear operation for a given time step. This calibration constant as defined exists for all radars. In the case of the KAZR, where pulse compression is used, a separate radar constant is required for each radar mode. Note that calculations are not always constant in time, as the transmitted radar power, the waveguide loss, and other factors may drift with environmental and/or radar stability changes.

MOSAiC calibrations posed new challenges when compared with the previous CACTI and COMBLE efforts because fewer techniques were applicable due to the primarily wintery environment and the remote mobile location of the campaign. MOSAiC focused on cross-calibration checks among all operational site radars.

1.2.2 Data Quality Masks

The radars measure not just hydrometeor backscatter, but are also sensitive to ground clutter, sea ice, sea clutter, insects, and extraneous radio frequency (RF) interference. To make the data more usable, masks that separate the hydrometeors from these non-meteorological signals are provided. This mask does not mean the data is “bad”, but rather provides an estimate of where the meteorological data are located. Because the processing and measured parameters vary for each radar, the masks available for each datastream will also vary.

1.2.3 Data Quality Corrections

In addition to calibration and data quality masks, other circumstances may cause poor-quality radar data. Sometimes, these issues (e.g., complete power/site outage) are not correctable, but several issues can be remedied. Wherever possible, b1 efforts correct for malfunctions or misconfigurations of the radar (e.g., as may still be found in a1 or b0 files). When a correction cannot be provided, data quality notes are appended to those data sets and/or described further in this report.

1.3 Radar Performance

During MOSAiC, the KAZR, MWACR, and KASACR operated for the entire campaign. As mentioned, the XSACR was unable to be operated once installed on the ship. Figure 4 shows the daily percentage of radar samples collected versus the maximum number expected. Radar operations were quite stable for the three remaining radars. The large down times in September and October 2019, and May and June 2020, were due to ship transit (i.e., the radars could not always be operated while the ship was in motion). The

August 2020 down time only affected the KASACR, as it was decided that the vertically pointing radars could continue to operate.

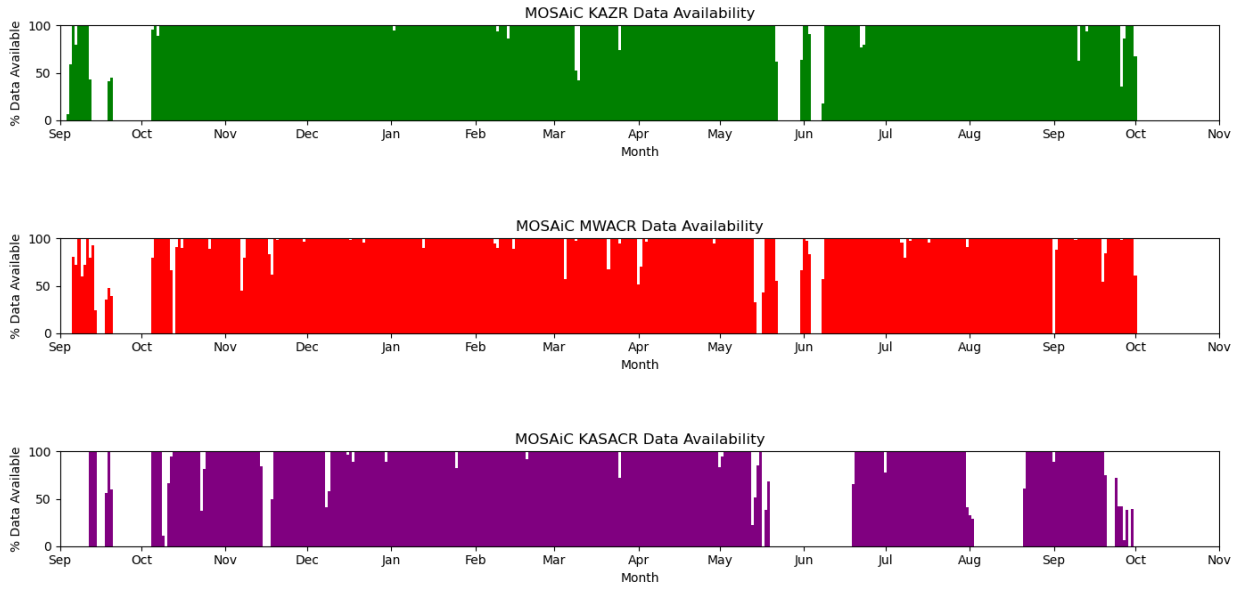

Figure 4. Radar data availability per day, as a percentage of expected operations.

1.4 Scan Strategy

The SACR deployed during MOSAiC operated only using two scanning modes: a plan position indicator scan, referred to as PPIV, and a hemispherical range height indicator scan, or HSRHI (Table 2). Due to the location on board the ship, the radar was unable to scan in vertically pointing mode. Additionally, the PPIs could only scan from 0 degrees to 270 degrees, while the HSRHIs could only scan to 90 degrees vertically to avoid scanning parts of the ship.

Table 2. Scan sequencing of ARM radars during MOSAiC.

PPIV Azimuth 0 - 280				HSRHI Elevation 0 - 90
Elevation	Elevation	Elevation	Elevation	Azimuth
0.0	2.5	6	25	90
0.5	3.0	9	36.5	150
1.0	3.5	14	60	120
2.0	4.5	19		180

2.0 Calibrations and Corrections

The calibration of the radars is a multi-part process consisting of tasks including onsite measurements as well as post-campaign data analysis such as cross-comparisons with other radars in the area. Due to the limitations imposed by this campaign's remote nature, certain techniques used in past ARM b1

calibration, monitoring, and conditioning efforts such as corner reflector scans, eRCA, and onsite measurements (i.e., comparisons with in situ disdrometer observations) could not be implemented. Therefore, radar calibrations during MOSAiC are based on relative calibration through radar cross-comparisons and long-term statistical expectations for radar cloud operations in similar regimes.

2.1 Techniques

Several techniques are used to calibrate and correct reflectivity-based variables, with an uncertainty of 2 to 3 dB. The following subsections describe the techniques and how they are applied to the radars.

2.2 KAZR Corrections

The KAZR operates using two different pulses, called its "GE" and "MD" modes. The first, GE or general mode, is a short pulse that provides returns near the ground and is sensitive to most cloud types. The second, MD or moderate mode, is a longer chirped pulse that provides a higher level of sensitivity, so it is more capable of seeing thinner clouds such as cirrus. However, the MD mode does have a larger blind range than GE mode because it cannot 'see' while it is transmitting, so misses the first 450 m above the radar.

This KAZR is single pol, so calibration focused on these two pulse modes reflectivity only. To achieve this, we compared the KAZR GE-mode reflectivities from MOSAiC to those from KAZRs at other ARM arctic locations, as well compared the GE and MD modes and cross-compared the GE mode with the KASACR.

2.2.1 KAZR Comparisons across ARM Locations

Because of the unique setting of the MOSAiC field campaign, limited methods were available to check the calibration of KAZR. As KAZR is one of the most stable radars operated by ARM, a comparison between the GE-mode reflectivity at MOSAiC and the GE-mode reflectivity at the ARM observatory NSA (North Slope of Alaska, near Utqiagvik, Alaska) was done through discussions with Sergey Matrosov, as shown in Figure 5. Here, you can see some variability month to month for reflectivities above each given threshold, but overall, they are within a few dB of each other. From this, we were able to confirm that the KAZR GE reflectivity data for MOSAiC is reasonably accurate, would not need any additional corrections, and could be used as the comparison point for the MWACR and KASACR. The adequacy of the MOSAiC KAZR GE-mode absolute calibration was also confirmed using a liquid water cloud microphysical process approach (Maahn et al. 2019) when analyzing KAZR observations of warm clouds (Matrosov et al. 2022).

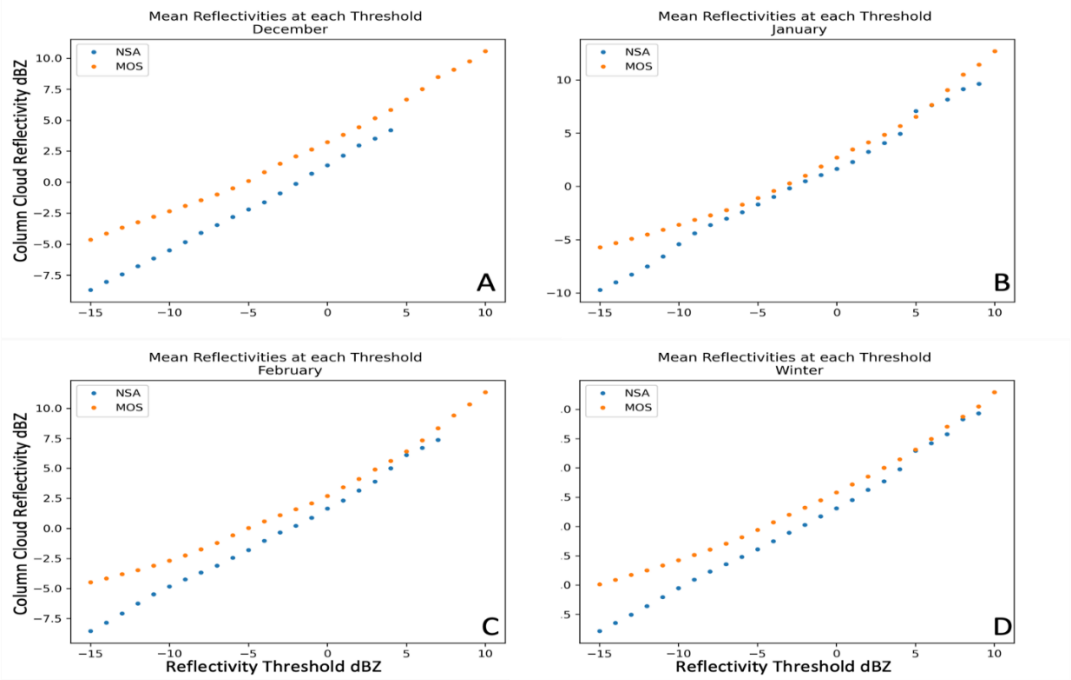

Figure 5. Monthly mean comparisons between NSA and MOS KAZR GE data for December (A), January (B), February (C), and combined (D).

2.2.2 Cross-Comparisons with KASACR

Once we had confirmed the KAZR GE reflectivities were reasonable in comparison with data from the NSA location, the KAZR GE and KASACR reflectivities were cross-compared using a subset of the HSRHI scans from the KASACR, as there were no vertically pointing scans for this campaign. Only the rays within one degree of vertical were used from the KASACR to compare with the KAZR. Because the two radars have different range grids, the KASACR rays were interpolated to a common range grid with KAZR. Visual inspection showed this interpolation had a negligible effect on the actual values.

Next, filters were applied to each radar to select only those points having solid meteorological signals as much as possible. The filters used were a signal-to-noise ratio (SNR) greater than 0 for both KAZR and KASACR, and reflectivities between -5 and 15 dBZ for KAZR only. The reflectivity filter was only used on the KAZR data because the discrepancies in reflectivity between the two radars were quite large; thus, KASACR often did not have cloud returns within that range. Only points chosen as "good" in both radars were used in the comparison, and a file was output containing the SACR file date and time, the mean offset, median offset, and number of points used in the comparison at that time-step.

The resulting offset between the general GE mode and the KASACR reflectivity varied throughout the campaign but hovered around -18 dB with a typical standard deviation of around 2dB (Figure 6). Because of the consistent change throughout the campaign, a polynomial curve fit was used to provide a daily offset value that could then be applied to the data, as in Figure 6. Between May 2020 and September 2020, the ship was often in motion and the radar powered down, causing gaps in the data. This also likely resulted in the data quality changes after the first shutdown in May; therefore, a second correction curve was used for the latter half of the campaign, shown in Figure 6. After correction, the offset between the two radars still had some variability, but the mean was much smaller, at around 1 dB.

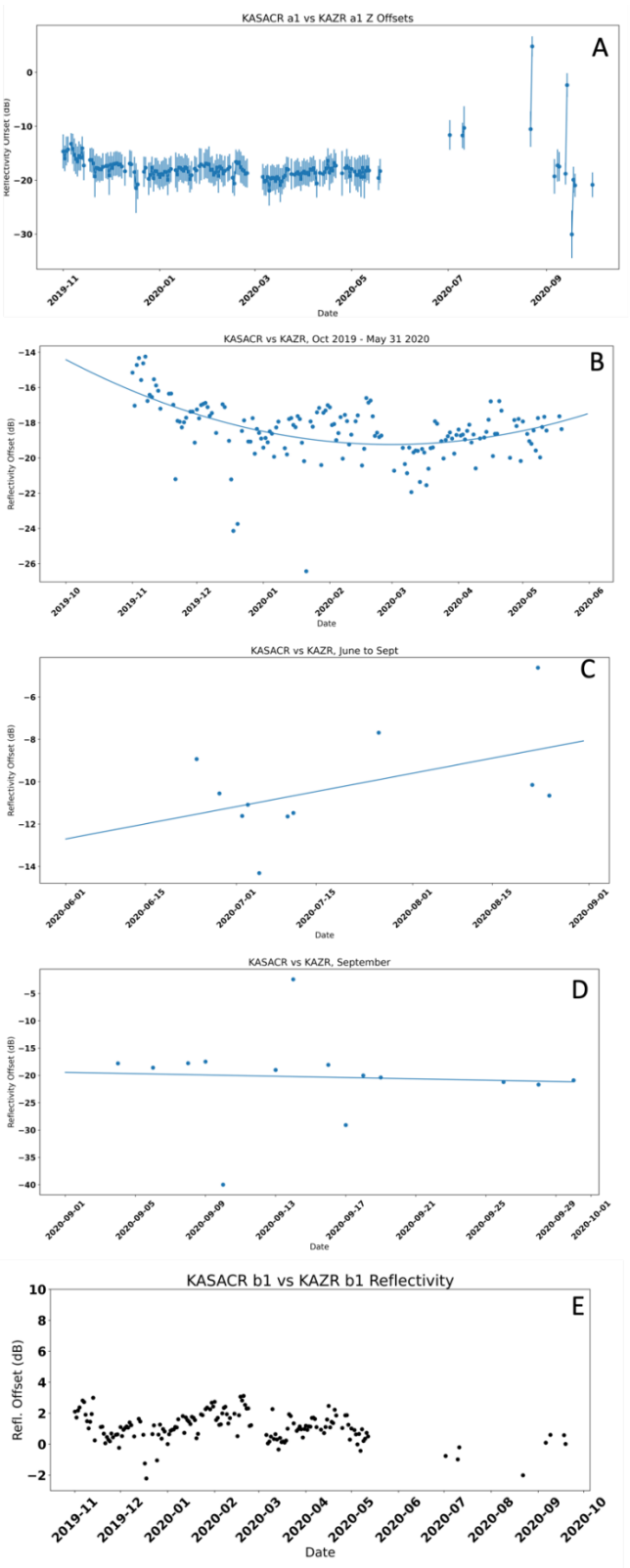

Figure 6. A shows the comparison between KASACR and KAZR prior to correction. B, C, and D show the correction curves applied to the reflectivity data. E shows the comparison after the KASACR reflectivity is correct.

2.2.3 Cross-Comparisons with MWACR

Next, the KAZR GE and MWACR reflectivities were cross-compared as both radars are vertically pointing and co-located. Because the two radars have different range grids, the MWACR rays were interpolated to a common range grid with KAZR. Visual inspection showed this interpolation once again had a negligible effect on the actual values.

Next, the same filters used in the comparison with KASACR were used. An output file containing the mean and median offsets, number of points used, and standard deviation was used to determine the differences between the radars.

The resulting offset between the general GE mode and the MWACR reflectivity varied throughout the campaign but was around -17 dB with a typical standard deviation of around 2dB (Figure 7). Because of the consistent change throughout the campaign, a polynomial curve fit was used to provide a daily offset value that could then be applied to the data, as shown in Figure 7. Between May 2020 and September 2020, the ship was often in transit; however, the MWACR and KAZR continued to operate for most of this time, so there are fewer data gaps. As a result, a single correction curve could be used for the data. After correction, the offset between the two radars still had some variability, but the mean was much smaller, at around -0.7 dB.

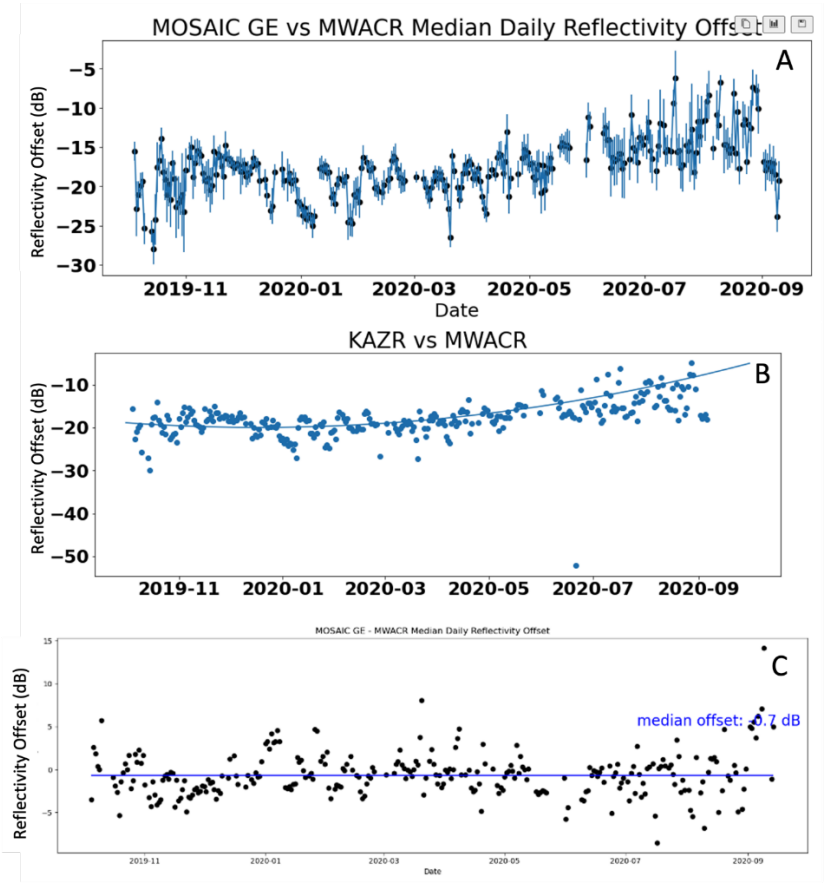

Figure 7. A shows the reflectivity comparison between MWACR and KAZR GE prior to correction, B shows the correction curve applied to the data, and C shows the reflectivity comparison after MWACR has been corrected.

2.2.4 KAZR Intermode Comparison

Finally, we can use the KAZR GE-mode reflectivity to compare with the moderate mode (MD)-reflectivity, following a similar method to the previous comparisons where we interpolated the GE data to match the MD data in both time and range, then used a filter of SNR > 0 and reflectivities between -5 and 15 dB for both the GE and MD data to determine the "good" points to be used for comparison. Once the output is plotted, we could see that the offset was higher than we typically see for our KAZR inter-mode comparison, at 4.8 dB (Figure 8), which was then applied to the data. The high variability early in the campaign was due to a loose waveguide screw and went away once it was tightened. Some of the other smaller variabilities during the campaign could be tied to snow buildup on the radome and would go away once the radome had been cleared off.

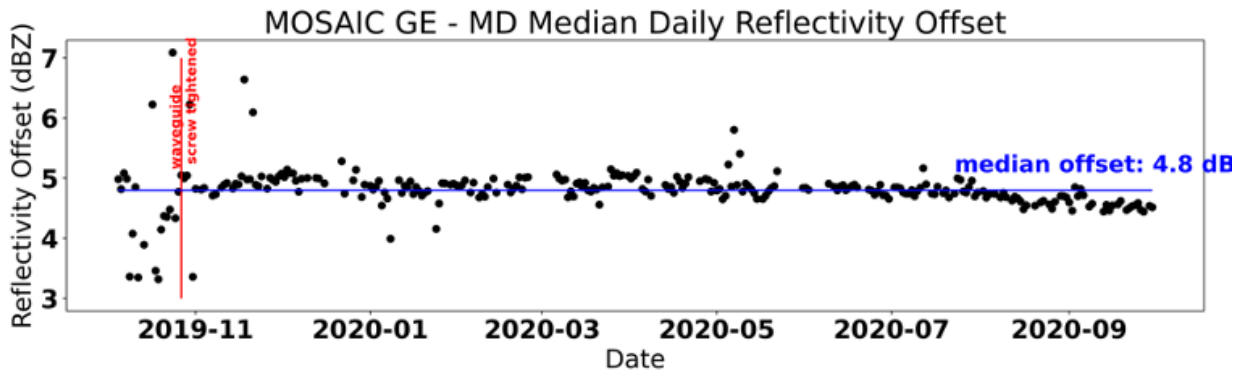

Figure 8. Comparison of reflectivity between the KAZR GE and MD modes.

2.2.5 KAZR MD Issue

The KAZR MD mode employs a pulse filter to create the shape of the long chirp pulse that makes its higher sensitivity possible. However, while the radar was in transit, the pulse filter parameters drifted from the original settings. The result was that spurious reflectivity is seen at ranges offset from the actual range location. These artifacts were problematic throughout the entire MOSAiC campaign in higher-reflectivity regions in the lowest 2-3 km. See Figure 9 for an example of this artifact, comparing returns from the KAZR MD mode and the unaffected KAZR GE mode. In general, it is best to use only the KAZR GE mode below approximately 3 km to avoid this artifact. A methodology for masking this MD artifact has been developed. It is not currently applied in the b1 data but can be provided upon request.

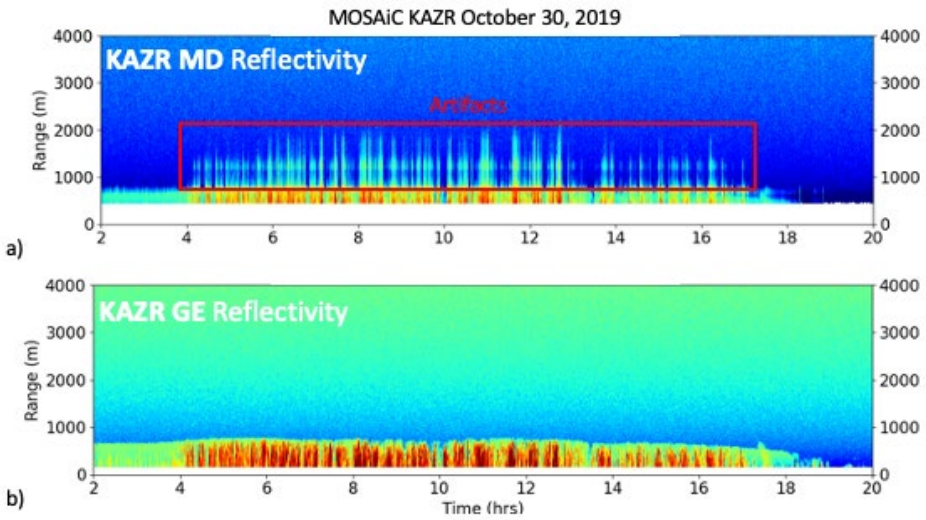

Figure 9. Time versus range image of KAZR Reflectivity on October 30, 2019 for A) MD mode, with spurious artifacts extending in range above high-reflectivity regions and B) GE mode, without artifacts.

3.0 Masks and Post-Processing

3.1 Meteorological Echo Mask

The SACR, KAZR, and MWACR do not contain any built-in masks, so simple meteorological echo masks were added to the b1 files. This mask was an SNR mask to help differentiate between meteorological returns and noise in the data, where an SNR > 0 is used as the differentiation point. Examples of this mask are shown in Figure 10.

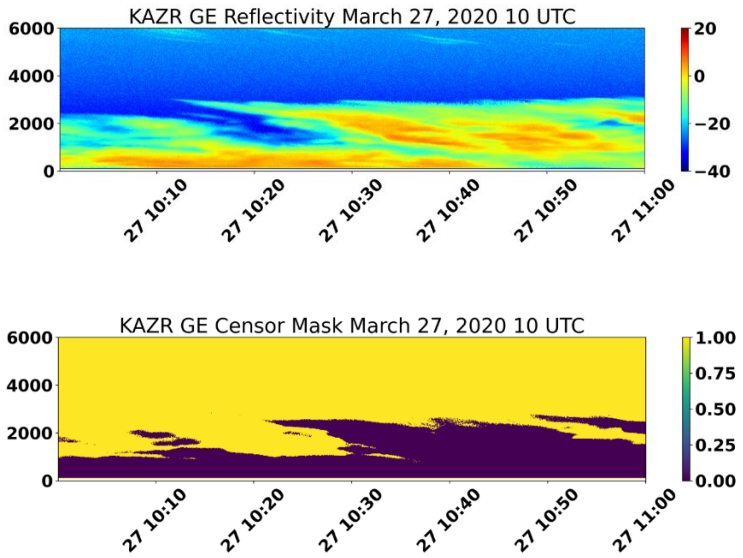

Figure 10. Example of the censor mask on the KAZR GE data from March 27, 2020 at 10 UTC. Top is the reflectivity; bottom is the censor mask where 0 is cloud and 1 is noise.

4.0 Description of Data Files

This section describes some of the more relevant parameters and variables in the radar datastreams (Table 3).

Table 3. Variables of SACR, KAZR, and MWACR.

Key
New variable calculated
Correction applied
New variable and correction applied

SACR File Contents	
Moments	
co_to_crosspol_correlation_coeff	Co-polar to cross-polar correlation coefficient (RhoXH)
crosspolar_differential_phase	Cross-polar propagation phase shift
linear_depolarization_ratio_v	Linear depolarization ratio, vertical channel
mean_doppler_velocity	Radial mean Doppler velocity, positive for motion away from the radar
Reflectivity	Equivalent reflectivity factor, with offset applied
signal_to_noise_ratio_copolar_h	Signal-to-noise ratio (SNR), horizontal channel
signal_to_noise_ratio_crosspolar_v	SNR, vertical channel
spectral_width	Spectral width
Masks	
censor_mask	Bit mask 0: no mask 1: SNR < 0
KAZR File Contents	
Moments	
linear_depolarization_ratio	All values set to nan. This variable is not present in this KAZR.
mean_doppler_velocity	Radial mean Doppler velocity, positive for motion away from the radar
mean_doppler_velocity_crosspolar_v	All values set to nan. This variable is not present in this KAZR.
reflectivity	Equivalent reflectivity factor, with offset applied
reflectivity_crosspolar_v	All values set to nan. This variable is not present in this KAZR.
signal_to_noise_ratio_copolar_h	SNR, horizontal channel
signal_to_noise_ratio_crosspolar_v	All values set to nan. This variable is not present in this KAZR.
spectral_width	Spectral width
spectral_width_crosspolar_v	All values set to nan. This variable is not present in this KAZR.

5.0 Ship Motion

The KAZR deployed during MOSAiC was equipped with an inclinometer, which provided a measurement of ship roll and pitch. During much of the deployment, it was not uncommon for KAZR to measure roll variations of two or more degrees over periods of a few minutes, even when the ship was not underway and presumably frozen in place. However, KAZR roll was stable (typically varying by less than half a degree over a day) from late December 2019 through mid-March 2020. Figure 11 shows a sample of roll variability on four dates.

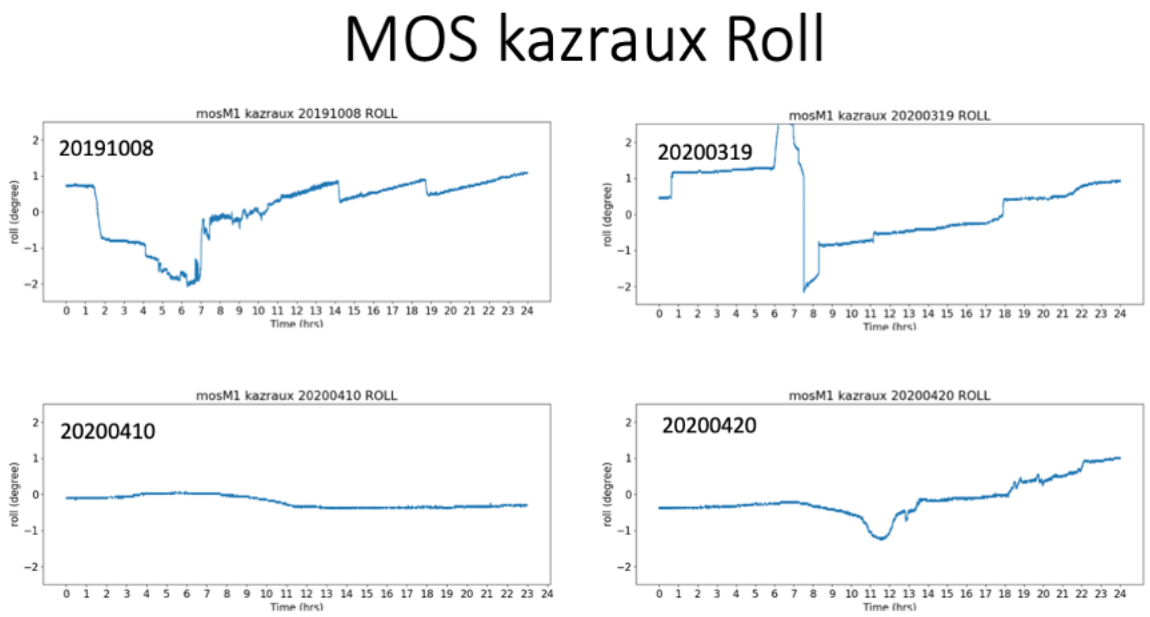

Figure 11. Ship roll angle versus time as measured by the KAZR inclinometer on four dates during the MOSAiC AMF deployment.

The pitch measured by the KAZR inclinometer is, predictably, much more constant while the ship was frozen in place. It varied significantly only while the ship was underway. This roll and pitch will also influence the Doppler information, such as the mean Doppler velocity, as it may not be pointing vertical if there were shifts in the ice or the *Polarstern* was in transit.

The impact of ship roll can be seen in KASACR scans, especially in HSRHI scans with elevation angles low enough to capture a ground clutter signal. When the ship has nonzero roll angle, SACR-detected ground clutter either appears at an elevation greater than zero degrees or does not appear in a sweep at all since the radar's lowest elevation angle is effectively looking above the surface. Figure 12 shows one example of the impact on a KASACR RHI image of a shift in roll of more than 3 degrees over a few minutes. The KASACR 0 degree azimuth corresponds to the bow of the ship for this campaign rather than North. Corrections to the KASACR elevation angle will be needed based on *Polarstern* roll angles but were not applied to the b1 data files. For information on the ship navigation, please use the ARM navigation datastream, mosnavM1.a1.

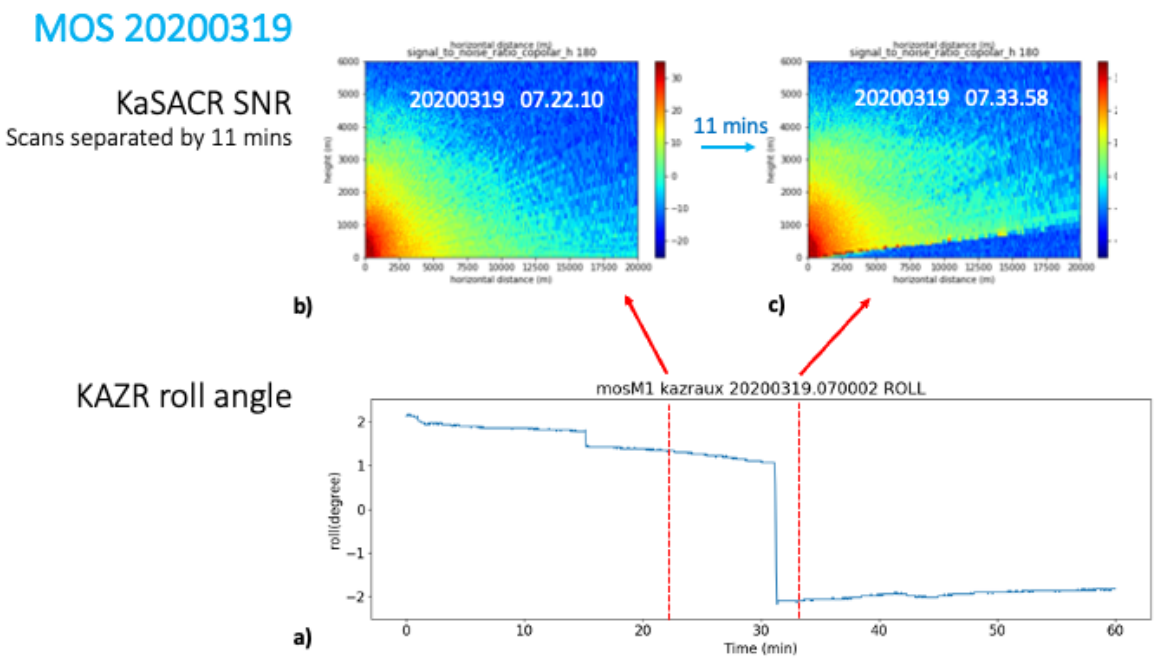

Figure 12. Impact of ship roll on ground clutter as seen by KASACR RHI sweep on March 19, 2020. A) Ship roll angle versus time over 60 minutes beginning at 07:00:02. B) KASACR signal-to-noise ratio RHI sweep with no evidence of ground clutter as recorded at 0.

6.0 References

ARM MOSAiC photos: https://www.flickr.com/photos/armgov/49429754988/in/album-72157708975573087/

ARM MOSAiC photos: https://www.flickr.com/photos/armgov/50192946938/in/album-72157708975573087/

Atmospheric Radiation Measurement (ARM) user facility. 2019. Navigational Location and Attitude (NAV). 2019-10-11 to 2020-10-01, ARM Mobile Facility (MOS) MOSAIC (Drifting Obs - Study of Arctic Climate); AMF2 (M1). Compiled by S. Walton. ARM Data Center. Data set accessed 2023-11-30 at http://dx.doi.org/10.5439/1974348

Hardin, JC, A Hunzinger, E Schuman, A Matthews, N Bharadwaj, A Varble, K Johnson, and SE Giangrande. 2020. CACTI Radar b1 Processing: Corrections, Calibrations, and Processing Report. U.S. Department of Energy. DOE/SC-ARM-TR-244. https://arm.gov/publications/brochures/doe-sc-arm-tr-244.pdf

Hunzinger, A, JC Hardin, N Bharadwaj, A Varble, and A Matthews. 2020. "An extended radar relative calibration adjustment (eRCA) technique for higher-frequency radars and range–height indicator (RHI) scans." *Atmospheric Measurement Techniques* 13(6): 3147–3166, https://doi.org/10.5194/amt-13-3147-2020

Johnson, K, T Fairless, and SE Giangrande. 2020. KA-Band ARM Zenith Radar Corrections (KAZRCOR, KAZRCFRCOR) Value-Added Products. U.S. Department of Energy. DOE/SC-ARM-TR-203. https://www.arm.gov/publications/tech_reports/doe-sc-arm-tr-203.pdf

Maahn, M, F Hoffmann, MD Shupe, G de Boer, SY Matrosov, and EP Luke. 2019. "Can liquid cloud microphysical processes be used for vertically pointing cloud radar calibration? *Atmospheric Measurement Techniques* 12(6): 3151–3171, https://doi.org/10.5194/amt-12-3151-2019

Matthews, A, A Hunzinger, K Johnson, E Schuman, Y-C Feng, JC Hardin, J Comstock, and SE Giangrande. 2023. COMBLE Radar b1 Processing: Corrections, Calibrations, and Processing Report. U.S. Department of Energy. DOE/SC-ARM-TR-285. https://www.arm.gov/publications/tech_reports/doe-sc-arm-tr-285.pdf

Matrosov, SY, MD Shupe, and T Uttal. 2022. "High temporal resolution estimates of Arctic snowfall rates emphasizing gauge and radar-based retrievals from the MOSAiC expedition." *Elementa: Science of the Anthropocene* 10(1): 00101, https://doi.org/10.1525/elementa.2021.00101

Shupe, MD, M Rex, B Blomquist, POG Persson, J Schmale, T Uttal, D Althausen H Angot, S Archer, L Bariteau, I Beck, J Bilberry, S Bucci, C Buck, M Boyer, Z Brasseur, IM Brooks, R Calmer, J Cassano, V Castro, D Chu, D Costa, CJ Cox, J Creamean, S Crewell, S Dahlke, E Damm, G de Boer, H Deckelmann, K Dethloff, M Dutsch, K Ebell, A Ehrliuch, J Ellis, R Engelmann, AA Fong, MM Frey, MR Gallagher, L Ganzeveld, R Gradinger, J Graeser, V Greenamyer, H Griesche, S Griffiths, J Hamilton, G Heinemann, D Helmig, A Herber, C Heuzé, J Hofer, T Houchens, D Howard, J Inoue, H-W Jacobi, R Jaiser, T Jokinen, O Jourdan, G Jozef, W King, A Kirchgaessner, M Klingebiel, M Krassovski, T Krumpen, A Lampert, W Landing, T Laurila, D Lawrence, M Lonardi, B Loose, C Lüupkes, M Maahn, A Macke, W Maslowski, C Marsay, M Maturilli, M Mech, S Morris, M Moser, M Nicolaus, P Ortega, J Osborn, F Patzold, DK Perovich, T Petäjä, C Pilz, R Pirazzini, K Posman, H Powers, KA Pratt, A Preuber, L Quelever, M Radenz, B Rabe, A Rinke, T Sachs, A Schulz, H Siebert, T Silva, A Solomon, A Sommerfeld, G Spreen, M Stephens, A Stohl, G Svensson, J Uin, J Viegas, C Voigt, P von der Gathen, B Wehner, JM Welker, M Wendisch, M Werner, Z Xie, and F Yue. 2022. "Overview of the MOSAiC expedition: Atmosphere." *Elementa: Science of the Anthropocene* 10.1: 00060, https://doi.org/10.1525/elementa.2021.00060

www.arm.gov

U.S. DEPARTMENT OF
ENERGY

Office of Science